Development of Feature Extraction for CT-scan Images in Detecting Auditory Ossicle Erosion

Yogi Wiyandra [1,*], Iskandar Fitri [2], and Yuhandri [2]

[1] Department of Computer System, Faculty of Computer Science,
University of Putra Indonesia YPTK, Padang, Indonesia
[2] Department of Information Technology, Faculty of Computer Science,
University of Putra Indonesia YPTK, Padang, Indonesia
Email: yogiwiyandra@upiyptk.ac.id (Y.W.); if@upiyptk.ac.id (I.F.); yuyu@upiyptk.ac.id (Y.)
*Corresponding author

***Abstract*—Infections of the ear, especially of the middle ear, which may result in the loss of the auditory bones, most commonly affect the hearing ability of man. This is because, in the middle part of a human's ear, these infections mainly result in the loss of three major auditory ossicles: malleus, incus, and stapes, which transmit sound vibrations from the tympanic membrane to the cochlea. Up to 60% of the hearing can be lost, with a harmful impact on human communication and interaction. Even though the examination is done through Computed Tomography (CT) scans, proper image interpretation is still essential for diagnoses. This project will research an advanced feature extraction method from the CT scan image to diagnose auditory bone erosion quickly. The research methodology of this project will be performed in several steps, which start from the input images and later include the pre-processing steps such as contrast stretching, cropping, re-sizing, filtering, contrast adjustment, and histogram equalization. The processing stage included object detection using the Region of Interest (ROI) method and shape extraction based on four parameters: area, perimeter, metric, and eccentricity. A novel algorithm had been designed purposely for shape extraction based on area parameters and was named the Chain Code algorithm; the method is named the MCACC method. Then, Experimental results demonstrate that from epoch 1, iteration 1, to epoch 100, iteration 100, the model achieves an accuracy rate of 97.37%. These findings highlight the efficacy of the MCACC algorithm in detecting erosion areas in auditory ossicles, providing a robust tool for medical imaging analysis. The detailed information regarding bone erosion with more explicit images obtained in this work significantly supports more advanced diagnosis and treatment in otolaryngology, thus enhances both patient care and communication capability.**

***Keywords*—feature extraction, extraction method, CT-scan image, ossicles erosion, auditory, Convolutional Neural Network (CNN), Chain Code (CC)**

I. Introduction

The human auditory system comprises organs responsible for hearing and balance. The ear is anatomically divided into three sections: the outer ear, the middle ear, and the inner ear. The outer ear includes the auricle (pinna), the external auditory canal, and the tympanic membrane (eardrum). The middle ear, or tympanic cavity, is an air-filled space situated within the petrous part of the temporal bone and houses the auditory ossicles [1].

In Fig. 1, the auditory system is depicted, illustrating the positions of the auditory ossicles, which are components of the middle ear (Malleus [2], Incus [3], and Stapes [4]). These ossicles may undergo erosion if the middle ear is affected by an infection. The method to diagnose whether the auditory ossicles have eroded due to a middle ear infection is by performing a Computed Tomography (CT) scan on the middle ear [5]. Fig. 2 presents an image produced by a CT scan, which is small and lacks sufficient detail to determine if there is erosion of the ossicles. Radiologists' observations indicate that the CT scan does not yet provide a clear image of the erosion occurring in the auditory ossicles. Physicians must meticulously analyze the CT scan results to render an accurate diagnosis based on the scan [6].

Fig. 1. Ossicles.

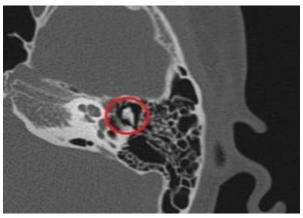

Fig. 2. CT-scan image of the auditory ossicles.

A lot of research has been carried out regarding improving or developing feature extraction in CT-scan images, as has been done by Wang *et al.* [7]. This study

Manuscript received July 4, 2024; revised August 14, 2024; accepted August 28, 2024; published December 23, 2024.

doi: 10.12720/jait.15.12.1380-1391

introduced a hybrid residual neural network with transfer learning to improve lung cancer subtype identification from CT scans. The model, fine-tuned on a proprietary dataset after pre-training on the LUNA16 dataset, achieved an accuracy of 85.71%. Next carried out by Nóbrega *et al.* [8]. This work utilized multiple deep learning architectures, including VGG16, MobileNet, and ResNet50, for classifying lung nodules. The Convolutional Neural Network-ResNet50 (CNN-ResNet50) and Support Vector Machine-Radial Basis Function (SVM-RBF) combination was particularly effective, achieving an accuracy of 88.41% and an Area Under the ROC Curve (AUC) of 93.19%. Similar research was also carried out by Li *et al.* [9]. This research evaluated a Deep Learning-based Computer-Aided Diagnosis (DL-CAD) system for detecting and characterizing lung nodules. The system, compared to double reading by radiologists, showed promising results, indicating the potential of deep learning models to enhance feature extraction and diagnostic accuracy in CT imaging.

Conceptually, this research involves the development of shape extraction techniques combined with a chain code algorithm applied to CT scan images. The purpose of developing these methods is to assess the extent of erosion in the auditory ossicles. This assessment is followed by a classification process that uses standards established by experts to categorize the ossicles as either normal or eroded, utilizing a Convolutional Neural Network (CNN) algorithm. This approach aids experts in making informed medical decisions. Practically, the research provides software that can be implemented in various Ear Nose Throat (ENT) clinics to identify patients with auditory ossicle erosion and take appropriate actions based on expert guidelines.

A significant amount of research has been conducted to improve or develop feature extraction in CT-scan images. For instance, Wang *et al.* [7] introduced a hybrid residual neural network with transfer learning to enhance lung cancer subtype identification from CT scans. Further research by Nóbrega *et al.* [8] utilized multiple deep learning architectures, including VGG16, MobileNet, and ResNet50, for classifying lung nodules. Additionally, Li *et al.* [9] evaluated a Deep Learning-based Computer-Aided Diagnosis (DL-CAD) system for detecting and characterizing lung nodules. These studies collectively highlight the advancements in feature extraction techniques from CT-scan images, driven by deep learning and machine learning methodologies. By incorporating these techniques, the current research aims to develop a robust and accurate system for assessing erosion in auditory ossicles, thereby providing valuable tools for medical professionals in diagnosing and treating middle ear infections.

The research is limited to developing form extraction to detect patients suffering from hearing bone erosion, thus obtaining a clearer image quality than before and conducting a comprehensive calculation process of erosion in the ear bone to determine the erosion of the auditory bone in accordance with the standards already submitted by experts by creating a new formula obtained from the spread of wide area formula in the extraction of the shape and Chain code named Multi Calculate Area Chain Code (MCACC). Subsequently, the condition of the hearing bones will be classified to determine normal and eroded auditory bones using the Convolutional Neural Network (CNN) algorithm.

The explanation above highlights one of the primary motivations for this research, which focuses on the erosion of the middle ear bones. This study is imperative due to the high incidence of middle ear infections that can lead to the erosion of the auditory ossicles, ultimately resulting in hearing loss. The research involves developing feature extraction methods to determine the area of erosion in the auditory ossicles. The objectives or the primary goal of the proposed method is achieved by deriving the formula for the area of shape extraction and Chain Code through implicit differentiation, named Multiple Calculate Area Chain Code (MCACC). We chose to develop the Chain Code method into MCACC which we proposed in this study because the method until now has not only calculated 8 connectivity areas in a measurement area. This study conducted a development so that the Chain Code method can perform calculations wider than 8 connectivity areas. Subsequently, the erosion of the auditory ossicles is classified using a Convolutional Neural Network (CNN) to determine whether the ossicles are normal or eroded, based on standards established by experts.

II. LITERATURE REVIEW

Research on Chain Code (CC) in 2021 [10] elaborates on the Normalized Differential Chain Code (NDCC) method for online recognition of handwritten Telugu characters. The formula employed in this method is based on the original Chain Code formula, utilizing features extracted by applying chain code to each character stroke. The dataset for this research comprises Telugu characters collected from 146 users, totaling 45,217 samples, and Bangla characters collected from 231 users, totaling 25,948 samples. The CC process in this research adheres to the Chain Code method, which intrinsically represents the shape of strokes. Each point on the stroke is encoded with a directional code based on the transition from one point to the next. This process enables the representation of stroke shape using a series of CC descriptors based on its starting point. The CC formula used incorporates 8-connectivity to encode the transitions between points. This directional code is represented by numbers from 0 to 7, indicating the relative transition direction from one point to the next.

Further development in the area of shape extraction has been presented by subsequent researchers, focusing on a static centroid location with varying contours based on point distribution. The calculated center of mass in this research remains static regardless of point distribution, as demonstrated by the application of absolute values in the developed area formula. The Chain Code (CC) process used in this research adheres to the CC method, employing 8-connectivity to encode transitions between points. A notable limitation of the formula used in this research is its sensitivity to the starting point and its lack of rotational invariance, resulting in varying CC values for the same object.

Another research in 2023 [11] The development of the area of shape extraction has also been explained by subsequent researchers who explain the development of shape extraction which focuses on the location of static centroids with contours that vary with the distribution of points. The position of the center of mass calculated in this study is static regardless of the point distribution conditions, this is proven by the application of absolute values in the development of the area formula used. Next reseach by Qi [6] conducted research on shape extraction is also narrated about the implementation of quantitative analysis to determine a good correlation between trends in several morphological characteristics and shape extraction which include area, diameter, roundness, consistency and entropy. The research was carried out by applying the standard formula used in shape extraction on transfer film.

III. Materials and Methods

A. Research Framework

This research framework is applied and carried out systematically, a guide for researchers in carrying out research so that the results obtained do not deviate from previously established objectives. The research framework designed in the research is as shown in Fig. 3 below:

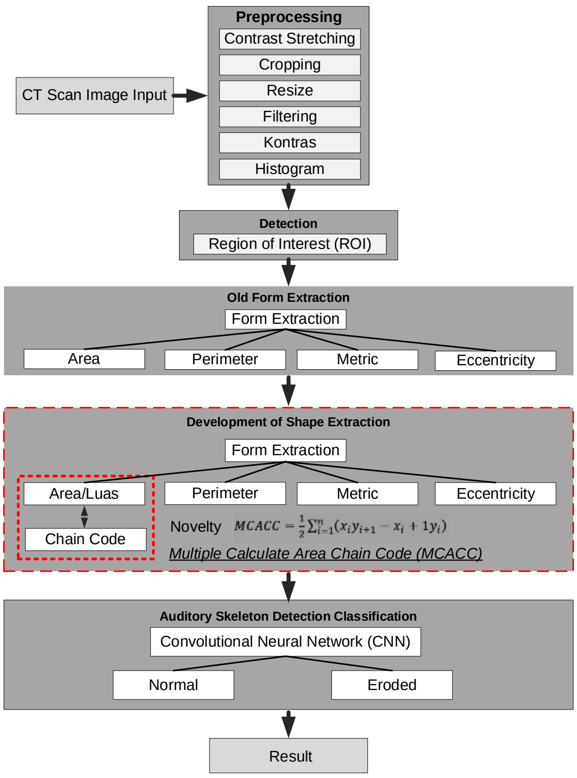

Fig. 3. Research framework.

The initial stage of this research framework involves inputting the images to be used in the processing [12, 13]. These images are sourced from CT scans of the auditory ossicles obtained directly from the radiology department [14]. The second stage involves preprocessing, which is the initial step in image processing. This includes applying contrast stretching to enhance image contrast. Subsequently, cropping is performed to ensure that the relevant part of the image is used, followed by resizing to obtain a clearer and more focused image. This is followed by filtering and adjusting the contrast to achieve the desired image quality, free from noise. The third stage aims to obtain a clearer image from the preprocessing steps. During the detection process, image processing using Region of Interest (ROI) is applied to separate the object from the background [15]. This is necessary because the object of interest is very small and needs to be isolated from irrelevant background elements. The fourth stage involves image processing to observe the erosion occurring in the auditory ossicles. This stage utilizes extraction methods, one of which is shape extraction. In this stage, a new algorithm is applied, combining it with the chain code algorithm on the area variable in shape extraction. This development aims to determine the extent of erosion in the auditory ossicles, enabling prompt and accurate intervention. The fifth stage of this research involves classifying the auditory ossicles that have undergone erosion using a Convolutional Neural Network (CNN). The final stage of this research provides information about the erosion that has occurred in the auditory ossicles.

B. Input Image CT Scan

The images utilized in this research are obtained from CT Scans (Computed Tomography Scans), a medical imaging technique that employs X-rays to generate detailed axial cross-sectional images of the body [16]. The collection of CT scan image data was performed at Dr. M. Djamil General Hospital in Padang. The dataset tested in this study comprises 100 CT scan images from 100 different patients. CT scans are frequently used in diagnosing and monitoring medical conditions, including cases of auditory ossicle erosion.

C. Preprocessing

Preprocessing is the initial stage of digital image processing, encompassing a series of techniques used to prepare the image before further analysis or processing [17]. The aim of preprocessing is to enhance image quality, remove noise, and improve the image's processing capability. The steps involved in preprocessing in this research are as follows:

1. Contrast Stretching: This method remaps the range of image intensity values so that the minimum and maximum intensity values are set to a larger range [18, 19]. Below is Pseudocode 1, which is used to perform contrast stretching:

Pseudocode 1. Contrast Stretching

Input: Img
Output: Show Contrast Stretching results
Initialization Img, bitdepth, m, n, i, j, x, slider_value
if bitdepth == 8
  image(i,j) = image(i,j) + slider_value;
if image(i,j) > 255
  image(i,j) = 255;
  end;

```
if image(i,j) < 0
   image(i,j) = 0;
   end;
elseif bitdepth == 24
   image(i,j,x) = image(i,j,x) + slider_value;
if image(i,j,x) > 255
   image(i,j,x) = 255;
   end;
if image(i,j,x) < 0
   image(i,j,x) = 0;
   end
end
```

2. Cropping: This process or technique is used to cut or select parts of the image that contain the desired area or object [20, 21]. Below is Pseudocode 2, used for cropping:

Pseudocode 2. Cropping

```
Input: Img
Output: Show Cropping Results
Initialization: Img, rect, position1, position2, rect1, rect2, x1, x2, widht1, widht2, object1, object2, round
rect1 = imrect;
position1 = wait(rect1);
x1 = round(position1(1));
y1 = round(position1(2));
rect2 = imrect;
position2 = wait(rect2);
x2 = round(position2(1));
y2 = round(position2(2));
object1 = imcrop(gambar, [x1, y1, width1, height1]);
object2 = imcrop(gambar, [x2, y2, width2, height2]);
```

3. Resizing: This stage involves changing the size of the image by altering the number of pixels. The pixel dimensions used in this research are 768 × 768 pixels [22, 23]. Below is Pseudocode 3, which is used for resizing:

Pseudocode 3. Resize

```
Input: object1, object2
Output: Show Resize Results
Initialization: object1, object2, y1, y2
y1 = imresize(object1,[768 768]);
y2 = imresize(object2,[768 768]);
```

4. Filtering is the process of modifying image pixels by applying a specific filter or kernel [24, 25]. The filtering stage employed in this research is the median filter, which functions to replace the intensity of a pixel with the median value of its neighboring pixels. Below is Pseudocode 4 used for filtering:

Pseudocode 4. Filtering

```
Input: y1, y2
Output: Show Filtering Results
Initialization: y1, y2, C, C1, noise, noise2, k, k2
C = rgb2gray(y1);
C1 = rgb2gray(y2);
noise1 = imnoise(C, 'Gaussian',0.01);
k1 = medfilt2(noise1);
noise2 = imnoise(C, 'Gaussian',0.01);
k2 = medfilt2(noise2);
```

5. Contrast enhancement in an image is a process used to improve image quality so that the information within the image can be better extracted [26, 27]. The process of adjusting contrast aims to produce a clearer and higher-quality image. Below is Pseudocode 5 used for contrast adjustment:

Pseudocode 5. Contrast

```
Input: k1, k2
Output: Show Contrast Results
Initialization: k1, k2, kont1, kont2
kont1 = imadjust(k1);
kont2 = imadjust(k2);
```

D. ROI (Region of Interest) Detection

In digital imaging, the Region of Interest (ROI) refers to a specific area within an image that is the primary focus for further analysis or processing [28]. Utilizing an ROI allows for the concentration of attention on the most relevant or significant parts of an image, thereby reducing the time and resources required to analyze or process the entire image. Below is Pseudocode 6 used for ROI detection:

Pseudocode 6. ROI Detection

```
Input: Img
Output: Show ROI Results
Initialization: Img, im_DIF, h_im, ROI, h, BW
Img = double
h = imrect;
setColor(h,'b')
mask = createMask(h);
BW = activecontour(Img,mask,1500); ROI = Img.*BW;
figure, imshow(ROI,[]);
im_DIF = Img-ROI;
Img = Img-ROI;
figure, imshow(im_DIF,[]);
ROI = uint8(ROI); im_DIF = uint8(im_DIF);
```

E. Shape Extraction

This research focuses on the development of an existing method within shape extraction techniques. Shape extraction techniques consist of four components: area, perimeter, metric, and eccentricity. The method developed in this research is the Chain Code method, which is used to extract the area value in shape extraction techniques. Below is an explanation of the shape extraction method prior to its enhancement into the improved shape extraction method.

1) Initial form extraction method (before developed)

The initial formula in determining the area using the chain code method by applying shape extraction is as follows [6]:

$$\sum_{i=p}^{n} U(x, y) \tag{1}$$

where: Σ = summation operator for all pixels, U = Coordinate (x, y), i = summation index used to determine the area, n = upper limit of the summation index, p = lower limit of the summation index.

The subsequent process in this stage involves reading the image using the chain code, beginning with the object's contour. This formula will be applied to the Chain Code algorithm [29]. In the initial Chain Code formula, the process detects the area using the chain code specifically for the erosion of the auditory ossicles, based on the object to be detected [30]. The formula used in this research has limitations, such as sensitivity to the starting point and lack of rotational invariance, resulting in varying chain code values for the same object, as illustrated in the following equation:

Code 0: Area = Area + y, Code 1: Area = Area + (y + 0.5), Code 2: Area = Area, Code 3: Area = Area – (y + 0.5), Code 4: Area = Area – y, Code 5: Area = Area – (y – 0.5), Code 6: Area = Area, Code 7: Area = Area + (y – 0.5).

The equation represents the process of contouring an object by using a series of numbers that indicate the direction of movement from one pixel to its neighboring pixel. The process of calculating the area of the object using Chain Code begins by identifying the rotational axis of the detected image. The initial formula used is as follows [6]:

$$Area = \frac{x + y + x_1}{2} \tag{2}$$

where: *Area*: The area of the image obtained using chain code, x: Number of horizontal pixels, y: Number of vertical pixels, x_1: Number of diagonal pixels.

The number of horizontal pixels is the count of pixels moving to the right or left (code 0 or 4). The number of vertical pixels is the count of pixels moving up or down (code 2 or 6). The number of diagonal pixels is the count of pixels moving diagonally (codes 1, 3, 5, or 7). Thus, the 0–7 shape extraction code can be explained as follows:

- Code 0 indicates a movement to the right by one pixel. The object area increases by the y-value of that pixel.
- Code 1 indicates a movement to the top-right by one pixel. The object area increases by the y-value of that pixel plus 0.5.
- Code 2 indicates a movement upward by one pixel. The object area does not change.
- Code 3 indicates a movement to the top-left by one pixel. The object area decreases by the y-value of that pixel plus 0.5.
- Code 4 indicates a movement to the left by one pixel. The object area decreases by the y-value of that pixel.
- Code 5 indicates a movement to the bottom-left by one pixel. The object area decreases by the y-value of that pixel minus 0.5.
- Code 6 indicates a movement downward by one pixel. The object area does not change.
- Code 7 indicates a movement to the bottom-right by one pixel. The object area increases by the y-value of that pixel minus 0.5.

The information derived from this process is obtained from the ROI-processed image [30]. This is followed by performing shape extraction to determine the characteristics of the auditory ossicles, such as area, perimeter, metric, and eccentricity. The shape extraction algorithm designed in this research is detailed in Algorithm 1.

2) New shape extraction method (after development)

The development of shape extraction is carried out by expanding the area of erosion occurring in the auditory ossicles using the Chain Code algorithm for image rotation reading [31]. The area determination process involves developing the area formula in shape extraction, using a standard formula commonly applied in image processing for binary images as per formula 1. The implicit differentiation derivative process is obtained from the chain code 0 value of the first equation, which will be implemented in the following equation [6]:

$$Area = Area + y \tag{3}$$

The development stages include integrating the original formula for area determination using shape extraction in object detection with the chain code. This involves expanding the area formula by breaking down each formula in the chain code to trace the object in the image and subsequently determining the area based on the newly created formula. The formula development process is conducted through implicit differentiation based on each coordinate value used in the chain code, such as determining the image movement direction starting from the right with a chain code value of 0, using the formula below [11]:

$$x_{i+1} - x_{i,} y_{i+1} - y_i = (+1, 0) \tag{4}$$

This formula was also developed by [11] to determine the area of an object but does not explain the objects inside the object. The resulting formula is like Eq. (5).

$$A = \frac{1}{2} \left| \sum_{i=0}^{M-1} x_i y_{i+1} - x_i + 1 y_i \right| \tag{5}$$

The formula consists of several variables, including coordinates (x, y) and their respective increments, with absolute values and multiplications involved in digital image processing. This serves to generate codes in the form of a series of numbers based on cardinal directions. This chain code can represent curves, lines, or contours of an area, determine the perimeter and area, and establish the shape factor of an object. The formula indicates that the parameter A represents the area of the object in the digital image. is the summation notation indicating that all values from i = 0 until $i = M - 1$. x_i and y_i are the coordinates of the point on the object for which the area is to be calculated. x_{i+1} and y_{i+1} are the coordinates of the next point on the object for which the area is to be calculated. $\frac{1}{2}$ is a constant used to calculate the area of the object. This formula functions to generate codes in the form of a series of numbers based on cardinal directions. This chain code can represent curves, lines, or contours of an area, determine the perimeter and area, and establish the shape factor of an object. Based on this formula, the initial chain code values vary for each image used, requiring an implicit differentiation process for each chain code coordinate so that the derivative results can interpret the chain code starting from 0 for various types of objects used.

In the implicit differentiation stage, two parameters tested within the image using the chain code are differentiated. Implicit differentiation is a technique based on the Chain Rule used to find derivatives when the relationship between variables is given implicitly rather than explicitly (solved for one variable in terms of another). To find the implicit derivative, take the derivative of both sides of the equation with respect to the independent variable, then solve for the derivative of the dependent variable with respect to the independent variable.

The first image is processed with respect to the x parameter and the second image with respect to the y parameter. These two parameters will be combined implicitly to obtain an optimal formula result called MCACC (Multiple Calculate Area Chain Code). The formula for the x parameter is derived as shown in Eq. (6).

$$\frac{\partial Area}{\partial x} = \frac{\partial}{\partial x}\left(\frac{1}{2}\left|\sum_{i=0}^{m-1}(x_i y_{i+1} - x_i + 1y_i)\right) + \frac{\partial}{\partial x}\left(\frac{1}{n-p+1}\sum_{i=p}^{n} U(x,y)\right) + \frac{\partial x}{\partial x}\right| \quad (6)$$

Calculation process $\frac{\partial Area}{\partial x}$ need to apply the chain rule in calculus. This equation is divided into two parts to simplify calculations. First part $\frac{\partial Area}{\partial x} = \frac{\partial}{\partial x}(\frac{1}{2}|\sum_{i=0}^{m-1}(x_i y_{i+1} - x_i + 1y_i))$ then proceed with the second calculation $\frac{\partial}{\partial x}(\frac{1}{n-p+1}\sum_{i=p}^{n} U(x,y)) + \frac{\partial x}{\partial x}|$. The first part uses the chain rule, we can calculate the partial derivative of each term in parentheses first. In this case, we only need to consider terms $x_{i,}y_{i+1} - x_i + y_i$. The second part needs to use the chain rule to calculate the derivative of $\sum_{i=p}^{n} U(x,y)$ However, as no information is provided about the function $U(x,y)$ cannot determine the partial derivative specifically. So, $\frac{\partial}{\partial y}(\frac{1}{n-p+1}\sum_{i=p}^{n} U(x,y)) + \frac{\partial x}{\partial x}|$ cannot be calculated without additional information from $U(x,y)$.

The y parameter in the Chain Code process will be derived using the initial area formula for shape extraction. The results of this formula are as in Eq. (7).

$$\frac{\partial Area}{\partial y} = \frac{\partial}{\partial y}\left(\frac{1}{2}\left|\sum_{i=0}^{m-1}(x_i y_{i+1} - x_i + 1y_i)\right) + \frac{\partial}{\partial y}\left(\frac{1}{n-p+1}\sum_{i=p}^{n} U(x,y)\right) + \frac{\partial y}{\partial y}\right| \quad (7)$$

The equation is divided into two parts to simplify analysis, the first part $\frac{\partial Area}{\partial y} = \frac{\partial}{\partial y}(\frac{1}{2}|\sum_{i=0}^{m-1}(x_i y_{i+1} - x_i + 1y_i))$ can apply the differentiation rule to each term in the number. In this case, we only need to consider terms containing the variable y. In the first term, y_{i+1} is the only term that contains y so we can take the derivative of that term $\frac{\partial}{\partial y} = (x_1 y_{i+1}) = x_1$.

Determining the area in shape extraction will be applied in the chain code to obtain an area that can be detected directly. This process represents a novel finding of this research, which will enable the direct detection of both the object and its area. The MCACC formula, applied in shape extraction and combined with the chain code process, is presented in Eq. (8).

$$MCACC = \frac{1}{2}\left|\sum_{i=1}^{m-1}(x_i y_{i+1} - x_i + 1y_i) + \frac{1}{n-p+1}\sum_{i=p}^{n} U(x,y) + y\right| \quad (8)$$

where: MCACC = Multiple Calculate Area Chain Code, Σ = Summation operator for all pixels, n = Number of sides of the object to be traced by the chain code on each of its sides, x_i = x-coordinate of the i-th point of the chain code to be used, y_i = y-coordinate of the i-th point of the chain code to be used, U = Coordinate point.

The source code of Eq. (8) can be seen in Pseudocode 7 below:

Pseudocode 7. MCACC (Multiple Calculate Area Chain Code)

Input: Img
Output: Show the area of the object
Initialization: Img, Object Area, Main Object Area, Chain Code, Contour, xref, yref, movement

```
for i = 1:length(contour)
if i == 1
prevPoint = contour(1, :);
  else
delta = contour(i, :) - prevPoint;
if all(delta == [1, 0])
chainCode(i) = 0;
  elseif all(delta == [1, –1])
    chainCode(i) = 1;
  elseif all(delta == [0, –1])
    chainCode(i) = 2;
  elseif all(delta == [–1, –1])
    chainCode(i) = 3;
  elseif all(delta == [–1, 0])
    chainCode(i) = 4;
  elseif all(delta == [–1, 1])
    chainCode(i) = 5;
  elseif all(delta == [0, 1])
    chainCode(i) = 6;
  elseif all(delta == [1, 1])
    chainCode(i) = 7;
end
  prevPoint = contour(i, :);
    end
  end
end
for i = 1:size(chainCode, 1)
movement = chainCode(i);
ObjectArea = ObjectArea + 1;
  if movement == 0|| movement == 1|| movement == 7
 yRef = yRef – 1;
  end
  if movement == 1|| movement == 2|| movement == 3
 xRef = xRef + 1;
  end
  if movement == 3|| movement == 4|| movement == 5
 yRef = yRef + 1;
  end
  if movement == 5|| movement == 6|| movement == 7
 xRef = xRef – 1;
  end
end

Detected Object Area = stats(1).Area;
disp([‘Main Object Area: ‘, num2str(Detected Object Area), ‘ pixel’]);
```

The chain code value displayed with various objects can read values starting from 0. This formula can provide more specific coordinate codes because it reads all the necessary directions in the image. This constitutes the novelty of the research, making it a significant finding. The algorithm used for image reading is as follows:

Algorithm 1: Shape Extraction Before Development

Input ROI Image
Read ROI Image
Display ROI Image
Initialize shape characteristic variables using the K-means clustering algorithm
Calculate (Area, Perimeter, Metric, Eccentricity)
Perform Shape Extraction
Display values (Area, Perimeter, Metric, Eccentricity)

Algorithm 2: Shape Extraction After Development (Chain Code)

Input Image
Convert to Bin ary Image
Obtain Contour with coordinates
Iterate through the contour
Determine the first chain code movement
Calculate the chain code movement direction
Iterate with the developed Chain Code
Calculate area from chain code values

F. Classification of Convolutional Neural Networks (CNN)

Classification at this stage involves categorizing or identifying specific objects or features within a digital image based on the characteristics of the auditory ossicles as defined by experts. One of the algorithms used in this classification process is the Convolutional Neural Network (CNN).

IV. Result and Discussion

A. Input CT Scan Image Results

The data focused on in this research includes 100 samples from different patients. The data processing involves both auditory ossicles, namely the right and left auditory ossicles. In total, 200 images are processed in the classification stage. The images data that we used is CT-Scan Images from ears of 100 patients right and left. However, for the application of the analysis results in this article, the focus will be on 4 CT scan images from 4 different patients used as samples in the study. Details regarding these 4 original CT scan input images can be seen in Table I below.

TABLE I. Input CT Scan Image Results

No	Input CT Scan Image	Information
1	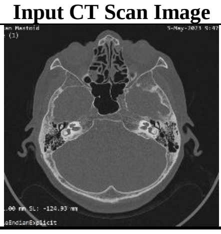	Patient 1
2		Patient 2
3		Patient 3
4		Patient 4

B. Preprocessing Result

1. The image resulting from contrast stretching is an enhanced CT scan input image. After this preprocessing step, the image becomes clearer and more detailed, leading to improved outcomes. This can be seen in Table II.
2. The image resulting from cropping is the portion of the image required for the study, based on the contrast-stretched result. Cropping aims to extract the necessary part of the image for the research while discarding the unnecessary parts. This process begins by determining the coordinates of the auditory ossicles, thus making it unnecessary to manually mark the object. The cropped preprocessed images can be seen in Table II, which includes images of both the left and right auditory ossicles.
3. The resized image is the cropped image adjusted to a standard size for this study. The cropping step produces two separate images of the left and right auditory ossicles. Due to their small size, these images are resized to facilitate further analysis. The resized preprocessed images can be seen in Table II.
4. The filtered image is the resized image that has undergone filtering to remove noise, resulting in a clean and clear image. This research employs the median filter method, replacing the pixel intensity with the median value of its neighboring pixels. The filtering process uses the Gaussian command to achieve the desired image clarity. The filtered preprocessed images can be seen in Table II.
5. The contrast-enhanced image is the filtered image with improved contrast, considered essential in image processing as it affects the visual quality. Brightness refers to the overall gray level in the image, adjusted by adding or subtracting pixel intensity values without altering the relative pixel ratios. The contrast-enhanced preprocessed images can be seen in Table II.

Table II presents data related to medical images of ossicles (small bones in the middle ear) from four patients. The table is divided into several columns, each showing different stages of image processing techniques applied to these ossicle images. The Table shows a well-structured approach to enhancing and processing medical images of ossicles. The sequential steps, from contrast stretching to cropping, resizing, filtering, and final contrast adjustment, result in images that are progressively clearer and more suitable for detailed analysis. Each processing step contributes to improving the visibility and clarity of the ossicles, which is crucial for medical diagnosis or research.

C. ROI Detection Result

The ROI image contains only the selected area (ROI) from the original image. This image differs in visual content and information from the original image because it focuses solely on a specific area. This approach is essential because using the ROI image allows for focused analysis or processing on the most relevant area of the image, often helping to improve the efficiency and accuracy of the image used. The results of the ROI process, ROI marking, and the resulting ROI image are presented in Table III.

TABLE II. IMAGE RESULTS FROM STRETCHING, CROPPING, RESIZING, FILTERING AND CONTRAST

Patient	Original Image	Contrast Stretching	Image of Ossicles Cropping		Image of Ossicles Resize		Image of Ossicles Filtering		Image of Ossicles Contrast	
			Right	*Left*	*Right*	*Left*	*Right*	*Left*	*Right*	*Left*
1										
2	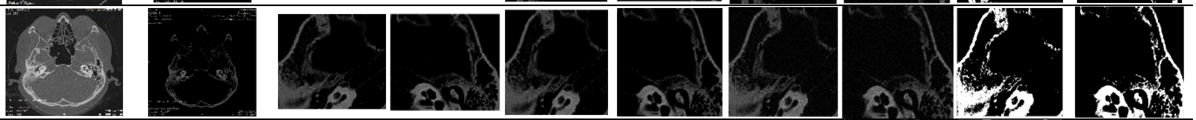									
3	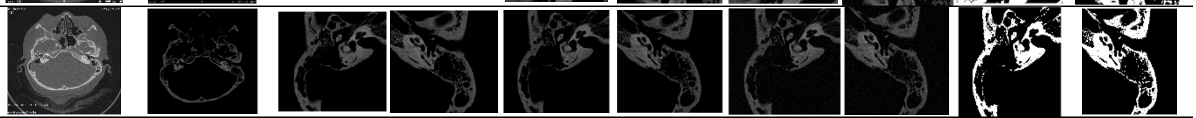									
4	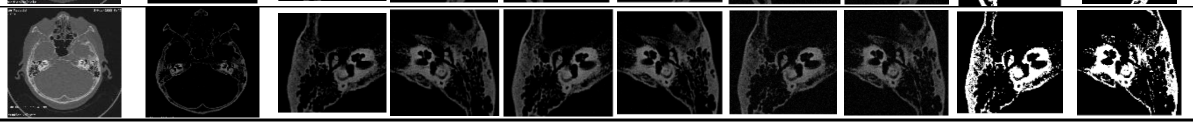									

TABLE III. CONTRAST RESULTS IMAGE, ROI MARKING AND ROI RESULTS

Patient	Image of Contrast		Image of ROI		Image ROI Result	
	Right	*Left*	*Right*	*Left*	*Right*	*Left*
1	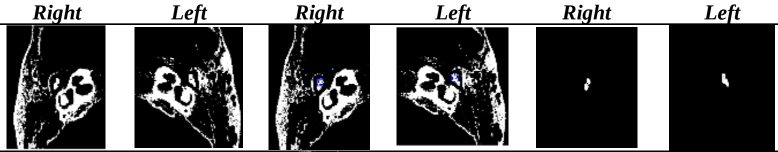					
2	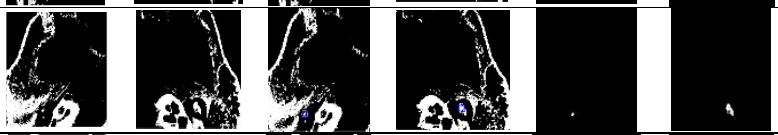					
3	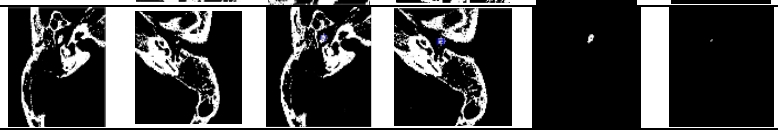					
4	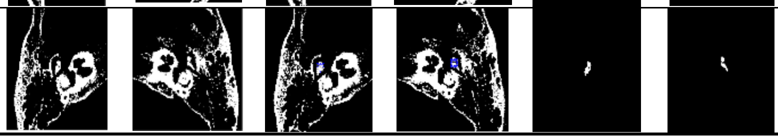					

Table III presents processed medical images focusing on the Region of Interest (ROI) in the ossicles of four patients. The table is divided into several columns showing different stages of image processing, particularly focusing on contrast enhancement, ROI identification, and the final ROI result. The table demonstrates a methodical approach to processing and analyzing ossicle images. The process begins with contrast enhancement, crucial for making the ossicles stand out against the background. Following this, ROIs are identified with clear markings, which are then isolated in the final step. Each stage appears to be crucial for narrowing down the images to the most relevant parts, making the process highly effective for medical research or diagnosis.

D. Form Extraction Results

1) Extraction results in the form of old extraction methods (before developed)

Several types of geometric shape extraction are performed, including determining the area to find the surface area of an image to be tested. This activity aims to measure the area of the object as the number of pixels within it. The perimeter is used as an alternative to measure the length of the object's edge. Eccentricity is used to determine how similar the object is to a circle, and the metric measures the ratio between the object's length and width. The results obtained at this stage are presented in Table IV.

TABLE IV. IMAGE OF EXTRACTION RESULTS IN THE FORM OF THE OLD EXTRACTION METHOD (BEFORE DEVELOPMENT) AND EXTRACTION IN THE FORM OF THE NEW EXTRACTION METHOD (AFTER DEVELOPMENT)

Patient	Information	Image	Extraction Results Form Extraction Method				
			Old (Before development)		New (After development)		
			Characteristic	Value	Chain Code	Area CC	Width of Erosion Area Detected
1	Right Ossicle	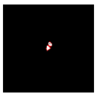	Area Perimeter Metric Eccentricity	1974 284.678 0.35943 0.90816	0554546532445553244544475446656566667540 7075465445432324533444434453454454545356 6655545076766776076617670076760777007 0771070012100101002223222176032243213 1 1243433532331007071217755770017110776 6 6076567756610210101022110212111002110 1 1223221017622131232543431444432453235 3 535544431	1,832.49	1. 0.5 2. 0.5 3. 0.6 4. 0.5 5. 0 6. 0.5 7. 0.5 8. 0.5 9. 4.47 10. 0.6
	Left Ossicle	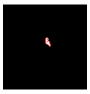	Area Perimeter Metric Eccentricity	2318 284.678 0.35943 0.90816	5445444345653555326675465666656555666700 0076560707717700700110070711717321770 7 6540776775676007600100760070176100766 6 6222176675000210775000010110076010731 0 0000223224333322432244433224443232322 1 2443133333232323233443232465443445453 2 44665324335535343553314	2,187.49	1. 13.98 2. 0.5 3. 0 4. 7.97 5. 0.5 6. 0.5 7. 0 8. 0.5 9. 0.5 10. 0.55 11. 0.5
2	Right Ossicle	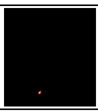	Area Perimeter Metric Eccentricity	324 96.142 0.44048 0.77842	0765540754444655475666075653255000010 7 0760177021112110121031021031543311434 3 535444443	277.49	-
	Left Ossicle	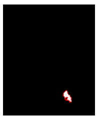	Area Perimeter Metric Eccentricity	2699 298.516 0.38061 0.87011	0546534444554554555340755555617654445 67 6757547670077210775561000717072176077 6 1017750777757760777210757007576007177 6 1707601171000717177021760070101211231 1 2653243121022435465322243333222212214 6 5323122222322333222443124453244475653 2 53432265431534331432324434553444434 4	2,553.49	1. 0.5 2. 0.5 3. 0.5 4. 0 5. 170.49 6. 0.5 7. 0.5 8. 0.5 9. 0 10. 0.6 11. 0.94 12. 0.5 13. 0.5
3	Right Ossicle	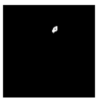	Area Perimeter Metric Eccentricity	1553 201.331 0.48146 0.85208	0544654544655433565444366656756655326 5 3532224654455545775076654676657566775 0 7700761071710002170107210707210071011 2 2117172232100022322172310111121121000 2 2213323245333353453445434 4	1,459.49	1. 0.5 2. 0.5 3. 0.5 4. 11.48 5. 0.94 6. 0.5 7. 0.66 8. 0.5 9. 0.5
	Left Ossicle	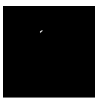	Area Perimeter Metric Eccentricity	225 79.362 0.44892 0.91143	0544575566654666535656576607751002171 2 1221021021111533102231224545 32	186.99	

4	Right Ossicle	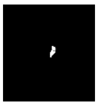	Area Perimeter Metric Eccentricity	2330 334.524 0.26164 0.91864	05546553253653253266553244356655465444332466534654465775675075765443310324366537544315324343345454545323755366534375407666567561777550776077676700217076700717000172172100072121077517217607000021010211000033110231110010210100173210321210101011002111022212344443232665555332214	2,180.49	1. 0.5 2. 0 3. 0.5 4. 0.53 5. 0.5 6. 0 7. 32.98 8. 9. 0.5 10. 0
	Left Ossicle	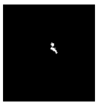	Area Perimeter Metric Eccentricity	1661 348.583 0.17178 0.93485	05454434444444535465566657675454323543432124315321445544343543534454444554560776565360076657007076667750001772100702173102101021021710721721775676754407675100077511077076653253560761117676553671010077000767117761717666076760010771170070322172444313124443343344322433233243234	1,500.99	1. 0.66 2. 0.5 3. 0.5 4. 0.5

2) Extraction results form a new extraction method (after being developed)

This stage describes the process of shape extraction combined with the chain code algorithm. The results obtained at this stage are shown in Table IV. The application of the chain code is described as an algorithm used to represent the contour of an object in the form of a chain code, which is used to calculate the object's area. First, the object's contour is converted into a chain code. In the image processing of auditory ossicle erosion, steps are taken to identify the ossicles experiencing erosion, followed by the area calculation process using the chain code, as shown in Table IV.

Table IV provides detailed results of the image extraction process using both old (before development) and new (after development) methods. Each row corresponds to different characteristics and measurements related to the ossicles (small bones in the ear) for individual patients. Here's an explanation of the key components, Patient Information, Area, Perimeter, Metric, Eccentricity, Chain Code and Area CC, Width of Erosion Area Detected. For each patient, the table compares the ossicle characteristics before and after the development of the new extraction method. The new method generally shows improvements in accuracy, consistency, and detection capabilities. For instance, the areas and perimeters are often closer to expected values, and the metrics indicate more reliable shape representations. This implies that the new extraction method enhances the ability to accurately analyze and diagnose ossicle conditions, providing better support for medical assessments and potential treatments.

E. Convolutional Neural Networks (CNN) Classification Results

The process carried out in this stage aims to clarify the operation of the image processed in shape extraction combined with the chain code. The resulting images will be processed using a Convolutional Neural Network (CNN) to determine the accuracy level of the processed images. Subsequently, classification layers such as the classificationLayer are used to calculate loss and enable model training for classification tasks.

Epoch	Iteration	Time Elapsed (hh:mm:ss)	Mini-batch Accuracy	Validation Accuracy	Mini-batch Loss	Validation Loss	Base Learning Rate
1	1	00:00:02	28.13%	57.89%	3.2549	0.7149	1.0000e-04
4	4	00:00:05	84.38%	86.84%	0.4968	0.5911	1.0000e-04
8	8	00:00:08	84.38%	86.84%	0.5803	0.4635	1.0000e-04
12	12	00:00:10	87.50%	89.47%	0.3071	0.2023	1.0000e-04
16	16	00:00:13	90.63%	89.47%	0.1395	0.1411	1.0000e-04
20	20	00:00:15	87.50%	97.37%	0.1539	0.1354	1.0000e-04
24	24	00:00:18	96.88%	97.37%	0.1501	0.1299	1.0000e-04
28	28	00:00:20	100.00%	97.37%	0.0967	0.1185	1.0000e-04
32	32	00:00:23	96.88%	97.37%	0.1190	0.1107	1.0000e-04
36	36	00:00:25	100.00%	97.37%	0.1010	0.1070	1.0000e-04
40	40	00:00:28	96.88%	97.37%	0.1101	0.1044	1.0000e-04
44	44	00:00:31	96.88%	97.37%	0.1075	0.0925	1.0000e-04
48	48	00:00:33	96.88%	97.37%	0.1134	0.0946	1.0000e-04
50	50	00:00:34	96.88%		0.0846		1.0000e-04
52	52	00:00:36	96.88%	97.37%	0.0743	0.0858	1.0000e-04
56	56	00:00:38	96.88%	97.37%	0.0942	0.0905	1.0000e-04
60	60	00:00:41	96.88%	97.37%	0.0925	0.0884	1.0000e-04
64	64	00:00:43	96.88%	97.37%	0.0894	0.0880	1.0000e-04
68	68	00:00:46	96.88%	97.37%	0.1005	0.0801	1.0000e-04
72	72	00:00:48	96.88%	97.37%	0.0810	0.0855	1.0000e-04
76	76	00:00:51	96.88%	97.37%	0.0969	0.0775	1.0000e-04
80	80	00:00:53	96.88%	97.37%	0.0844	0.0806	1.0000e-04
84	84	00:00:56	96.88%	97.37%	0.0944	0.0794	1.0000e-04
88	88	00:00:58	96.88%	97.37%	0.0823	0.0770	1.0000e-04
92	92	00:01:01	96.88%	97.37%	0.0886	0.0770	1.0000e-04
96	96	00:01:04	96.88%	97.37%	0.0814	0.0741	1.0000e-04
100	100	00:01:06	96.88%	97.37%	0.0801	0.0732	1.0000e-04

Akurasi: 97.3684%

Fig. 4. CNN classification accuracy results.

Fig. 4 presents the classification results of a Convolutional Neural Network (CNN) across multiple epochs and iterations. Each row represents the performance metrics for a specific epoch, detailing the progress of the network training. The key metrics include: Epoch and Iteration, Time Elapsed, Mini-batch Accuracy and Loss Validation Accuracy and Loss, Base Learning Rate. The results indicate a steady improvement in both mini-batch and validation accuracy over epochs, suggesting effective learning and generalization. The validation accuracy stabilizes around 97.37%, indicating a well-trained model with good predictive performance. The base learning rate remains constant, implying no dynamic adjustments were made during this training phase. Overall, the table provides a comprehensive view of the training dynamics and performance of the CNN model, demonstrating its robustness and reliability in classification tasks. The accuracy achieved reflects the model's effectiveness in learning from the training data and accurately predicting the validation dataset.

The relationship of the result of Table IV with Fig. 4 are:

1. Application of CNN in Image Processing: The CNN model could be used to classify and segment the ossicle images, which is the initial step before extracting detailed features such as area, perimeter, and eccentricity. The training and validation accuracy and loss metrics from the CNN results table indicate how well the model performs in identifying and classifying different regions of the ossicle images.

2. Improved Extraction Methods: The development of a new extraction method, as indicated in Table IV, might involve the application of advanced image processing techniques, possibly including CNNs, to enhance the accuracy of the feature extraction. The comparison of old and new methods in Table IV shows improvements that could be attributed to more sophisticated preprocessing and classification algorithms, potentially including CNN-based segmentation.
3. Validation of Extraction Results: The validation accuracy and loss metrics from the CNN results can be correlated with the improved feature extraction outcomes shown in Table IV. High validation accuracy in the CNN model suggests that the model effectively generalizes to new, unseen ossicle images, leading to more accurate and consistent extraction results in the new method.

The CNN classification results provide a foundation for understanding the performance of the image analysis model, which is crucial for accurately identifying and classifying regions in ossicle images. Table IV then shows the practical application of these methods, demonstrating improvements in feature extraction after developing new techniques, possibly including CNN-based approaches. Together, they highlight the effectiveness of CNNs in enhancing image processing tasks, leading to better diagnostic tools and outcomes in medical image analysis.

V. Conclusion

The MCACC algorithm offers precise information on object images, consistently reading chain code values with a constant value of 0 across all image types. This capability ensures that the MCACC algorithm accurately reads the detected area by combining the chain code area and the shape extraction area. This development significantly contributes to the detection of auditory ossicle erosion with enhanced accuracy and clarity. Experimental results demonstrate that from epoch 1, iteration 1, to epoch 100, iteration 100, the model achieves an accuracy rate of 97.37%. These findings highlight the efficacy of the MCACC algorithm in detecting erosion areas in auditory ossicles, providing a robust tool for medical imaging analysis. Future research should focus on developing a mobile application that users can access anytime and anywhere. This application would enable the processing of CT scans and the retrieval of images directly from the radiology department. Such a development would facilitate direct discussions of results with experts and doctors specializing in ENT, thereby enhancing the clinical utility of the MCACC algorithm. In conclusion, the MCACC algorithm represents a significant advancement in the field of medical imaging, offering precise and efficient detection of auditory ossicle erosion. The high accuracy rate observed in experimental trials underscores its potential for clinical application.

Conflict of Interest

The authors declare no conflict of interest.

Author Contributions

Y.W. conducted the research; I.F. analyzed the data; Y. wrote the paper; all authors had approved the final version.

Acknowledgment

We express our deepest thanks to Universitas Putra Indonesia YPTK Padang for facilitating this research activity and to the Yayasan Perguruan Tinggi Komputer (YPTK) Padang for funding this research activity.

References

[1] M. Hassoun *et al.*, "Tumors of the nervous system and hearing loss: Beyond vestibular schwannomas," *Hear. Res.*, 2024. doi: 10.1016/j.chest.2024.03.018

[2] J. O. Hansen and S. Foghsgaard, "Bone cement repair of malleus handle fractures: Intraoperative video and case report of two patients," *Am. J. Otolaryngol.—Head Neck Med. Surg.*, vol. 45, no. 3, pp. 1–3, 2024. doi: 10.1016/j.amjoto.2024.104256

[3] K. Mantsopoulos *et al.*, "Hydroxyapatite bone cement in the reconstruction of defects of the long process of the incus: Personal experience and literature review," *Am. J. Otolaryngol.—Head Neck Med. Surg.*, vol. 42, no. 4, 103002, 2021. doi: 10.1016/j.amjoto.2021.103002

[4] M. Teschner, T. Lenarz, and S. Busch, "Results of a new Vibrant Soundbridge stapes head coupler after subtotal petrosectomy," *Otolaryngol. Case Reports*, vol. 23, no. 2, 100402, 2022. doi: 10.1016/j.xocr.2022.100402

[5] T. Shimura *et al.*, "A case of a patient with IgG4+ plasma cell infiltration, an IgG4-related disease, localized to the auditory ossicles," *Otolaryngol. Case Reports*, vol. 24, no. 5, 100443, 2022. doi: 10.1016/j.xocr.2022.100443

[6] Y. Qi *et al.*, "Quantitative measurement of morphological characteristics of PTFE composite Transfer films based on computer graphics," *Materials (Basel)*, vol. 16, no. 4, 2023. doi: 10.3390/ma16041688

[7] R. Shah and S. N. A. Parveen, "An extensive review on lung cancer diagnosis using machine learning techniques on radiological data: State-of-the-art and perspectives," *Arch. Comput. Methods Eng.*, vol. 30, no. 11, pp. 4917–4930, 2023. doi: https://doi.org/10.1007/s11831-023-09964-3

[8] P. K. Pagadala, S. L. Pinapatruni, C. R. Kumar, S. Katakam, L. S. K. Peri, and D. A. Reddy, "Enhancing lung cancer detection from lung CT scan using image processing and deep neural networks," *Rev. Intelligence Artif.*, vol. 37, no. 6, pp. 1597–1605, 2023. doi: 10.18280/ria.370624

[9] R. Hosseini, S. H., Monsefi and S. Shadroo, "Deep learning applications for lung cancer diagnosis: A systematic review," *Multimed. Tools Appl.*, vol. 83, no. 07, pp. 14305–14335, 2024. https://doi.org/10.1007/s11042-023-16046-w

[10] S. Inuganti and R. R. Ramisetty, "Online handwritten Telugu character recognition using normalized differential chain code feature," *Webology*, vol. 18, pp. 1–15, 2021. doi: 10.14704/WEB/V18SI04/WEB18110

[11] J. Chaki and N. Dey, *A Beginner's Guide to Image Shape Feature Extraction Techniques*, 1st ed. Boca Raton: CRC Press, 2019. https://doi.org/10.1201/9780429287794

[12] W. Cowger, A. Gray, S. H. Christiansen, H. DeFrond, A. D. Deshpande, L. Hemabessiere, and S. Primpke, "Critical review of processing and classification techniques for images and spectra in microplastic research," *Applied Spectroscopy*, vol. 74, no. 9, pp. 989–1010, 2020.

[13] S. Chong, M. Momin, and A. Narayan, "A research framework to analyse visual persuasion of photographs in sustainability reports, " *Meditari Accountancy Research*, vol. 31, no. 5, pp. 1453–1482, 2023.

[14] I. Krebbers, R. M. V. D. Goor, R. J. W. V. Kampen, P. H. M. H. Theunissen, and V. E. Bergshoeff, "An unexpected, invasive disease of the mastoid bone and external auditory canal," *Otolaryngol. Case Reports*, vol. 15, no. 4, pp. 8–10, 2020. doi: 10.1016/j.xocr.2020.100169

[15] D. Gowda *et al.*, "A novel method of data compression using ROI

for biomedical 2D images," *Meas. Sensors*, vol. 24, no. 8, 100439, 2022. doi: 10.1016/j.measen.2022.100439

[16] Y. Yanagisawa, M. Yoshida, M. Doi, T. Hoshino, Y. Inoue, and M. Yamazaki, "Retroperitoneal abscess associated with closed pelvic ring fracture diagnosed by fine free air on initial trauma pan computed tomography scan," *Trauma Case Reports*, vol. 51, no. 4, 101031, 2024. doi: 10.1016/j.tcr.2024.101031

[17] L. Dular, F. Pernuš, and Ž. Špiclin, "Extensive T1-weighted MRI preprocessing improves generalizability of deep brain age prediction models," *bioRxiv Prepr. Serv. Biol.*, vol. 173, no. 2, 2023. doi: 10.1016/j.compbiomed.2024.108320

[18] A. Javaid, M. Sadiq, and F. Akram, "Skin cancer classification using image processing and machine learning," in *Proc. 18th Int. Bhurban Conf. Appl. Sci. Technol. IBCAST 2021*, no. 2, 2021, pp. 439–444. doi: 10.1109/IBCAST51254.2021.9393198

[19] A. Rehman, M. A. Khan, Z. Mehmood, T. Saba, M. Sardaraz, and M. Rashid, "Microscopic melanoma detection and classification: A framework of pixel-based fusion and multilevel features reduction," *Microsc. Res. Tech.*, vol. 83, no. 4, pp. 410–423, 2020. doi: 10.1002/jemt.23429

[20] A. S. Paymode and V. B. Malode, "Transfer learning for multi-crop leaf disease image classification using convolutional neural network VGG," *Artif. Intell. Agric.*, vol. 6, pp. 23–33, 2022. doi: 10.1016/j.aiia.2021.12.002

[21] P. Deng, Z. Jiang, H. Ma, Y. Rao, and W. Zhang, "Improving crop image recognition performance using pseudolabels," *Inf. Process. Agric.*, no. 2, 2024. doi: 10.1016/j.inpa.2024.02.001

[22] S. Avidan and A. Shamir, "Seam carving for content-aware image resizing," in *Proc. ACM SIGGRAPH Conf. Comput. Graph.*, vol. 26, no. 3, 2022. doi: 10.1145/1275808.1276390

[23] A. Fajar, R. Sarno, C. Fatichah, and A. Fahmi, "Reconstructing and resizing 3D images from DICOM files," *J. King Saud Univ.—Comput. Inf. Sci.*, vol. 34, no. 6, pp. 3517–3526, 2022. doi: 10.1016/j.jksuci.2020.12.004

[24] S. Moran, P. Marza, S. McDonagh, S. Parisot, and G. Slabaugh, "Deeplpf: Deep local parametric filters for image enhancement," *Proc. IEEE Comput. Soc. Conf. Comput. Vis. Pattern Recognit.*, pp. 12823–12832, 2020. doi: 10.1109/CVPR42600.2020.01284

[25] B. Kim, J. Ponce, and B. Ham, "Deformable kernel networks for joint image filtering," *Int. J. Comput. Vis.*, vol. 129, no. 2, pp. 579–600, 2021. doi: 10.1007/s11263-020-01386-z

[26] D. Vijayalakshmi, M. K. Nath, and O. P. Acharya, *A Comprehensive Survey on Image Contrast Enhancement Techniques in Spatial Domain*, vol. 21, no. 1. Springer US, 2020. doi: 10.1007/s11220-020-00305-3

[27] Y. Lu, S. Young, H. Wang, and N. Wijewardane, "Robust plant segmentation of color images based on image contrast optimization," *Comput. Electron. Agric.*, vol. 193, 2022. doi: 10.1016/j.compag.2022.106711

[28] K. Prabhavathi, M. B. Anandaraju, and V. Ravi, "Region based medical image encryption using advanced zigzag transform and 2D logistic sine map (2DLSM)," *Int. J. Cogn. Comput. Eng.*, vol. 4, no. June, pp. 349–362, 2023. doi: 10.1016/j.ijcce.2023.10.001

[29] F. Ramezanzadeh and H. Shokrzadeh, "Efficient routing method for IoT networks using bee colony and hierarchical chain clustering algorithm," *e-Prime—Adv. Electr. Eng. Electron. Energy*, vol. 7, no. 8, 100424, 2024. doi: 10.1016/j.prime.2024.100424

[30] Irawanda, "Application of chain code algorithm for feature extraction of vehicle plate image objects," *J. Informatics Manag. Inf. Technol.*, vol. 1, no. 1, pp. 30–33, 2021.

[31] A. babaeinesami, P. Ghasemi, M. Abolghasemian, and A. P. chobar, "A Stackelberg game for closed-loop supply chains under uncertainty with genetic algorithm and gray wolf optimization," *Supply Chain Anal.*, vol. 4, no. 8, 100040, 2023. doi: 10.1016/j.sca.2023.100040